

GSFC/TM-1998-206646



Global Warming Estimation From Microwave Sounding Unit

C. Prabhakara, Goddard Space Flight Center, Greenbelt, MD

R. Iacovazzi Jr., Raytheon STX Corporation, Greenbelt, MD

J.-M. Yoo, Ewha Womans University, Seoul, South Korea

G. Dalu, CNR, Cagliari, Italy

National Aeronautics and
Space Administration

Goddard Space Flight Center
Greenbelt, Maryland 20771

February 1998

Available from:

NASA Center for Aerospace Information
800 Elkridge Landing Road
Linthicum Heights, MD 21090-2934
Price Code: A17

National Technical Information Service
5285 Port Royal Road
Springfield, VA 22161
Price Code: A10

ABSTRACT

Microwave Sounding Unit (MSU) Ch 2 data sets, collected from sequential, polar-orbiting, Sun-synchronous National Oceanic and Atmospheric Administration (NOAA) operational satellites, contain systematic calibration errors that are coupled to the diurnal temperature cycle over the globe. Since these *coupled errors* in MSU data differ between successive satellites, it is necessary to make compensatory adjustments to these multisatellite data sets in order to determine long-term global temperature change. With the aid of the observations during overlapping periods of successive satellites, we can determine such adjustments and use them to account for the *coupled errors* in the long-term time series of MSU Ch 2 global temperature. In turn, these adjusted MSU Ch 2 data sets can be used to yield global temperature trend.

In a pioneering study, Spencer and Christy (SC) (1990) developed a procedure to derive the global temperature trend from MSU Ch 2 data. In their procedure, the magnitude of the *coupled errors* is not determined explicitly. Furthermore, based on some assumptions, these *coupled errors* are eliminated in three separate steps. Such a procedure can leave unaccounted residual errors in the time series of the temperature *anomalies* deduced by SC, which could lead to a spurious long-term temperature trend derived from their analysis. In the present study, we have developed a method that avoids the shortcomings of the SC procedure. Based on our analysis, we find there is a global warming of 0.23 ± 0.12 K between 1980 and 1991. Also, in this study, the time series of global temperature *anomalies* constructed by removing the global mean annual temperature cycle compares favorably with a similar time series obtained from conventional observations of temperature.

Contents

LIST OF FIGURES	vii
LIST OF TABLES	viii
LIST OF SYMBOLS	ix
1. INTRODUCTION	1
2. DATA ANALYSIS	
2.1 Selection of data	2
2.2 Nature of the coupled errors in MSU data	3
2.3 Rectification of MSU Ch 2 data	8
2.4 Error analysis of MSU Ch 2 data	10
2.5 Global temperature change and trend from MSU Ch2	12
3. CONCLUSIONS	14

FIGURES

Figure 1. Percentage of Land, Ocean, and Land-Ocean Sum in each latitudinal belt from 75N to 75S. The percentage in each belt constituted by coastal grid boxes is given by $(100 - \text{Land-Ocean Sum})$	3
Figure 2a. Annual temperature cycle over the global land for 1982 deduced from NOAA 6 in MSU Ch 1 at 7:30 a.m. and 7:30 p.m., and from NOAA 7 for the local times 2:30 a.m. and 2:30 p.m. b) Diurnal cycle over global land for January 1982, and c) for July 1982	4
Figures 3a, 3b, and 3c. Same as figures 2a, 2b, and 2c, except for MSU Ch 1 data over global ocean	5
Figures 4a, 4b, and 4c. Same as figures 2a, 2b, and 2c, except for MSU Ch 2 data over global land	6
Figures 5a, 5b, and 5c. Same as figures 2a, 2b, and 2c, except for MSU Ch 2 data over global ocean	7
Figure 6a. Difference between MSU Ch 2 monthly mean temperature of NOAA 7 and NOAA 6 satellites, deduced from the overlap data for 1982	10
Figure 6b. Same as figure 6a, except for NOAA 11 and NOAA 10 satellites, for 1990	12
Figure 7. Corrected MSU Ch 2 global temperature as a function of time. Solid lines correspond to the scale on the left ordinate and represent global mean temperature deduced from successive satellites (6, 7, 9, 10, and 11) covering the period 1980–1991. The MSU observed warming from 1980 to 1991 is 0.23 ± 0.12 K (refer to text). Open circles correspond to the scale on the right ordinate and denote monthly temperature anomalies with respect to the 12-year mean annual cycle	13

TABLES

Table 1. Details of satellite data used in the present analysis	8
Table 2a. Unadjusted average Ch 2 temperature (K) data over global land. (Add 200 to the temperature given in table.)	9
Table 2b. Unadjusted average Ch 2 temperature (K) data over global ocean. (Add 200 to the temperature given in table.)	9
Table 3a. Global land MSU Ch 2 temperature measurements and <i>coupled errors</i> (K). Included are observations before and after correction $\sum(-\Delta\bar{T}_m)$ for <i>coupled errors</i> . (Add 200 to the mean temperature values, \bar{T}_m and $\hat{\bar{T}}_m$, given in table.)	11
Table 3b. Global ocean MSU Ch 2 temperature measurements and <i>coupled errors</i> (K). Included are observations before and after correction $\sum(-\Delta\bar{T}_m)$ for <i>coupled errors</i> . (Add 200 to the mean temperature values, \bar{T}_m and $\hat{\bar{T}}_m$, given in table.)	11

SYMBOLS

w_{ij}	Weight applied to the data in a grid box having indices i, j
T_{AM}'	MSU Ch 2 global monthly mean brightness temperature obtained by averaging the data measured close to 7:30 a.m. or 2:30 a.m. local time
T_{PM}'	MSU Ch 2 global monthly mean brightness temperature obtained by averaging the data measured close to 7:30 p.m. or 2:30 p.m. local time
\bar{T}_{AM}	MSU Ch 2 global multiyear mean brightness temperature obtained by averaging the \bar{T}_{AM}' data
\bar{T}_{PM}	MSU Ch 2 global multiyear mean brightness temperature obtained by averaging the \bar{T}_{PM}' data
\bar{T}_m	Unadjusted average of \bar{T}_{AM} and \bar{T}_{PM}
$\Delta\bar{T}_m$	Difference between the average temperature of two overlapping successive satellites
$\hat{\bar{T}}_m$	Adjusted average temperature of \bar{T}_{AM} and \bar{T}_{PM}
\bar{T}_0	Initial MSU Ch 2 temperature of the globe
\bar{T}_f	Final MSU Ch 2 adjusted temperature of the globe
$\sigma'_o, \sigma'_L, \text{ and } \sigma'_g$	<i>Coupled errors</i> over the global ocean, global land, and the globe
$\sigma_o, \sigma_L, \text{ and } \sigma_g$	Total errors over the global ocean, global land, and the globe

1. INTRODUCTION

Temperature observations made from satellites orbiting around the Earth can be valuable to studies of global temperature and its variation with time, because of the uniformity of global measurements made by them. However, necessary accuracy in the data and in the method of its analysis should be maintained to get good results. With such measurements, global temperature could be monitored readily, which could help assess the impact of anthropogenic effects.

Passive infrared radiometer temperature observations made from satellites are contaminated by clouds in the troposphere. Therefore, these observations are not helpful to monitor global temperature change, which can be on the order of 0.1 K in a decade. In a pioneering study, Spencer and Christy (SC) (1990) demonstrated in a preliminary way the potential of the passive microwave radiometers to monitor global temperature with that precision. In particular, they emphasize that Microwave Sounding Unit¹ Ch 2 near 53.74 GHz, because of its weak sensitivity to hydrometeors in the atmosphere and very strong response to thermal state, provides measurements that reflect basically the temperature of the midtroposphere, which is closely related to the surface air temperature.

The global temperature trend deduced from MSU data by SC disagrees with that obtained from conventional data analysis, which is mainly based on surface air temperature or radiosonde-observed temperature (Hansen and Lebedeff, 1987; Jones et al., 1986; Angell, 1988; Oort and Liu, 1993). The global temperature trend derived by SC (1992) from MSU Ch 2 data is near zero (~ 0.03 K) during the time period 1979–1990. On the other hand, the conventional data analyses show a warming of about 0.2 K during this period. This disagreement has led to a careful examination of the analysis of SC by Hansen and Wilson (1993), Trenberth and Hurrell (1996), Prabhakara et al. (1995), and Shah and Rind (1995). Utilizing the radiosonde data, Hansen and Wilson simulated theoretically a time series of Ch 2 global temperature from 1979 to 1991 and calculated the resulting temperature trend. Based on their study, they indicate the analysis of SC underestimates the global temperature trend. Trenberth and Hurrell contend that the limited amount of overlap data used to calculate intersatellite calibration corrections can introduce errors in the analysis of SC. Prabhakara et al. suggest that there is nonnegligible residual

hydrometeor contamination in the MSU Ch 2 data, which has not been screened by SC; and that this residual contamination could effect the resulting trend. Shah and Rind emphasize noise introduced by the surface conditions. The above critical examinations did not reveal the key weakness in SC's satellite data analysis. In this study, we find there is a weakness in the SC treatment of the diurnal effects and the calibration errors. When this weakness is removed, the satellite observations indicate a global warming in the period 1980–1991 of about 0.23 ± 0.12 K.

If the long-time series of successive NOAA operational satellites had the same Sun-synchronous orbital geometry over the globe and contained no errors, it would be a relatively simple matter to get the time series of the global mean temperature from MSU Ch 2 data. However, this is not so. There are two different orbital geometries for NOAA satellites. One of them has local equatorial crossing times set close to 7:30 a.m. and 7:30 p.m., while the other has these local times set close to 2:30 a.m. and 2:30 p.m. A satellite with the first orbital geometry is referred to as a "morning satellite," while a satellite with the second geometry is called an "afternoon satellite."

Sometimes, a morning satellite is followed by an afternoon satellite. This introduces significant problems in developing a time series of MSU Ch 2 temperature data that can be analyzed to get a long-term trend. First, there can be differences in the Ch 2 temperature of the successive satellites because of the diurnal cycle. Secondly, the calibration of the MSU data between the two successive satellites could differ. These two errors exist in the MSU data as *coupled errors*. To eliminate these *coupled errors*, Spencer et al. (1991) developed a procedure which depends crucially on the temperature *anomalies* with respect to a suitable mean annual cycle in Ch 2 temperature data. The three steps involved in this procedure are described below.

First, for each latitude belt the NOAA 6 1982 mean annual cycle is subtracted from the MSU Ch 2 data of all the morning satellites to get the zonal temperature anomalies of the morning satellites, while the NOAA 7 1982 mean annual cycle is subtracted from the MSU Ch 2 data of the afternoon satellites to get the temperature anomalies of the

¹ Microwave Sounding Unit flown on Sun-synchronous, polar-orbiting NOAA operational satellites

afternoon satellites. These anomalies are properly weighted and integrated to get global anomalies. It is assumed that the diurnal cycle effect is removed in this step. In the second step, the temperature *anomalies* obtained from the overlapping data from two successive satellites are equalized with the help of an adjustment term. From this step, it is assumed that the intersatellite calibration errors are removed. In the final step, the temperature *anomaly* time series obtained as a result of the two previous steps is refined by subtracting an improved mean annual cycle. This procedure involves a chain of subtractions to get the final anomaly time series. We find that the long-term global temperature trend derived from this final time series does not account fully for the *coupled errors* in the MSU Ch 2 data.

The objective of the present study is to deduce global temperature from the MSU Ch 2 data, using an independent approach. For this purpose, we have to understand the nature of the *coupled errors* present in the MSU data, so that we can explicitly adjust the data for these errors. Then we will develop a method, based on the MSU Ch 2 global temperature data (not the temperature *anomalies*), to determine the trend.

2. DATA ANALYSIS

2.1 Selection of data

The MSU is a cross-track scanning instrument that makes 11 observations along each scan (NOAA, 1991). In the present study, we have selected only the measurements made by the MSU in the nadir direction. This choice reduces the number of observations, but it also avoids the need to empirically relate the cross-track scan data to the data along nadir direction, as done by SC (1992).

Outliers in the MSU Ch 2 brightness temperature data are eliminated. Whenever this temperature exceeds 300 K, or is less than 200 K, we neglect such data. Such outliers constitute less than 1% of the entire data set.

For each month from 1980 to 1991, the MSU nadir data has been binned into 2° latitude x 3° longitude grid boxes over the globe. The data set from the morning satellites is separated into two global sets by the satellite equatorial crossing local time. Thus, one set corresponds closely to the 7:30 a.m. equatorial crossing local time and the other set closely to the 7:30 p.m. equatorial crossing local time. Similarly, the afternoon satellite data set is partitioned into

two global data sets by the 2:30 a.m. and the 2:30 p.m. equatorial crossing local times. This step of the analysis reveals that, because of the orbital configuration of the polar-orbiting NOAA operational satellites, for each 2° x 3° grid box near the equator there is a maximum possible number of 7 MSU Ch 2 nadir observations in a given month at each of the four local equatorial crossing times. This number increases away from the equator. Subsequently, a monthly average of these observations, for each month and in each grid box, is formed separately for the 7:30 a.m. and the 7:30 p.m. local times for the morning satellites. Similarly, for the afternoon satellites, grid box monthly averages are formed separately for the 2:30 a.m. and the 2:30 p.m. local times.

For the purpose of our analysis, the MSU data in the 2° x 3° grid boxes are separated into global land and ocean areas. Data from the grid boxes that form the coastal regions are not considered in the analysis. The data loss due to coastal rejection does not exceed 20% in the 60N to 60S zone, as shown in figure 1; and only in limited parts of the high latitudes does the rejected coastal data exceed 20%. The total land plus ocean area considered in our analysis amounts to 84% of the area from 75N to 75S, of which the land accounts for 27% and the ocean accounts for 57%. This rejection of coastal data does not bias the global proportion of ocean and land areas.

We have not eliminated any of the MSU Ch 2 data for hydrometeor contamination, because the interannual error in MSU Ch 2 data introduced by this contamination over the globe, ~0.04 K (Prabhakara et al., 1995) is much smaller than other errors in the MSU data.

There are deficiencies in the Ch 2 global monthly mean temperatures of the following months: March 1980, June 1982, Dec. 1982, Sept. 1984, Feb. 1988, Dec. 1988, and Feb. 1989. These deficiencies arise due to unusually long time gaps in the MSU data set, or when there are significant numbers of questionable data within a given month that are close to, but within, the limits of the outlier rejection. Based on first and second order derivatives, these deficiencies are remedied by interpolation of the time series of the Ch 2 global monthly mean temperature.

The monthly population of the Ch 2 nadir data in a grid box for a particular time of the satellite orbit may not appear large; but we find it is adequate. This is due to the fact that our analysis depends on multiyear average temperature, and

not the anomaly of the monthly average temperature, on a global scale. Temperature change over a long period, or its time trend, is deduced in our study from the multiyear averages over the global ocean and the global land.

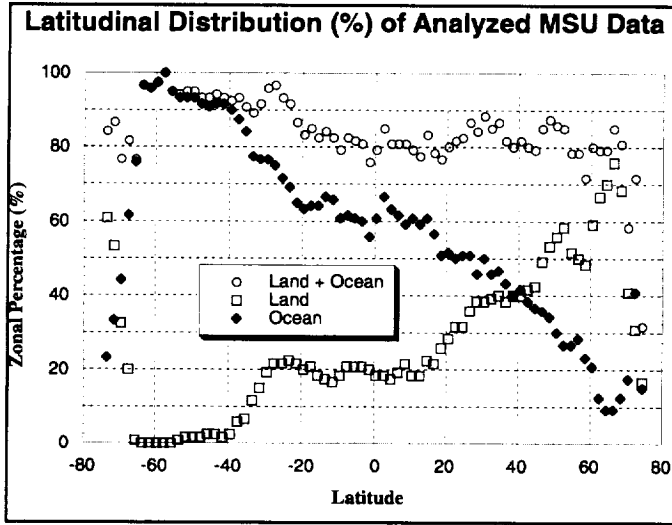


Figure 1. Percentage of Land, Ocean, and Land-Ocean Sum in each latitudinal belt from 75N to 75S. The percentage in each belt constituted by coastal grid boxes is given by (100 - Land-Ocean Sum).

2.2 Nature of the *coupled errors* in MSU data

A thorough discussion of the MSU calibration procedure, utilized to get NOAA operational data sets, is outside the scope of this study, but a brief description of this procedure is given here. In this calibration procedure, the temperatures of the onboard warm black body (~288 K) and free space (~2.7 K) are first taken as references. Then, a given radiometer reading of a target on the Earth is converted into a brightness temperature using a calibration procedure provided by NOAA (1997).

From the earlier description of the satellite orbital geometry of the morning and afternoon satellites, we note that whenever both morning and afternoon satellites are observing the Earth, such observations made by those satellites in a month can be partitioned into four sets based on each local equatorial crossing time of the orbits. We expect that these four sets of data will reflect the phase and amplitude of the global diurnal temperature cycle, if there are no calibration errors in the observations of the two satellites. However, since there are calibration errors, the diurnal temperature cycle in these data will be distorted. Because the variations of temperature in the diurnal cycle are

superimposed on the calibration errors, at present the magnitude of either the diurnal effect or the calibration errors cannot be assessed individually. For this reason, these *coupled errors* have to be treated as one entity.

In order to understand the nature of these *coupled errors*, we have analyzed the MSU Ch 1 and Ch 2 temperature data, obtained from overlapping NOAA 6 and NOAA 7 satellites, separately over the global land and ocean areas for 1982. MSU Ch 1 observations (50.3 GHz) lie in the window region of the 60 GHz oxygen absorption band, so they can provide information that supports and supplements the information given by Ch 2 data. The MSU Ch 1 or Ch 2 global monthly mean temperature \bar{T}_{AM} for a given period is calculated using the following numerical equation:

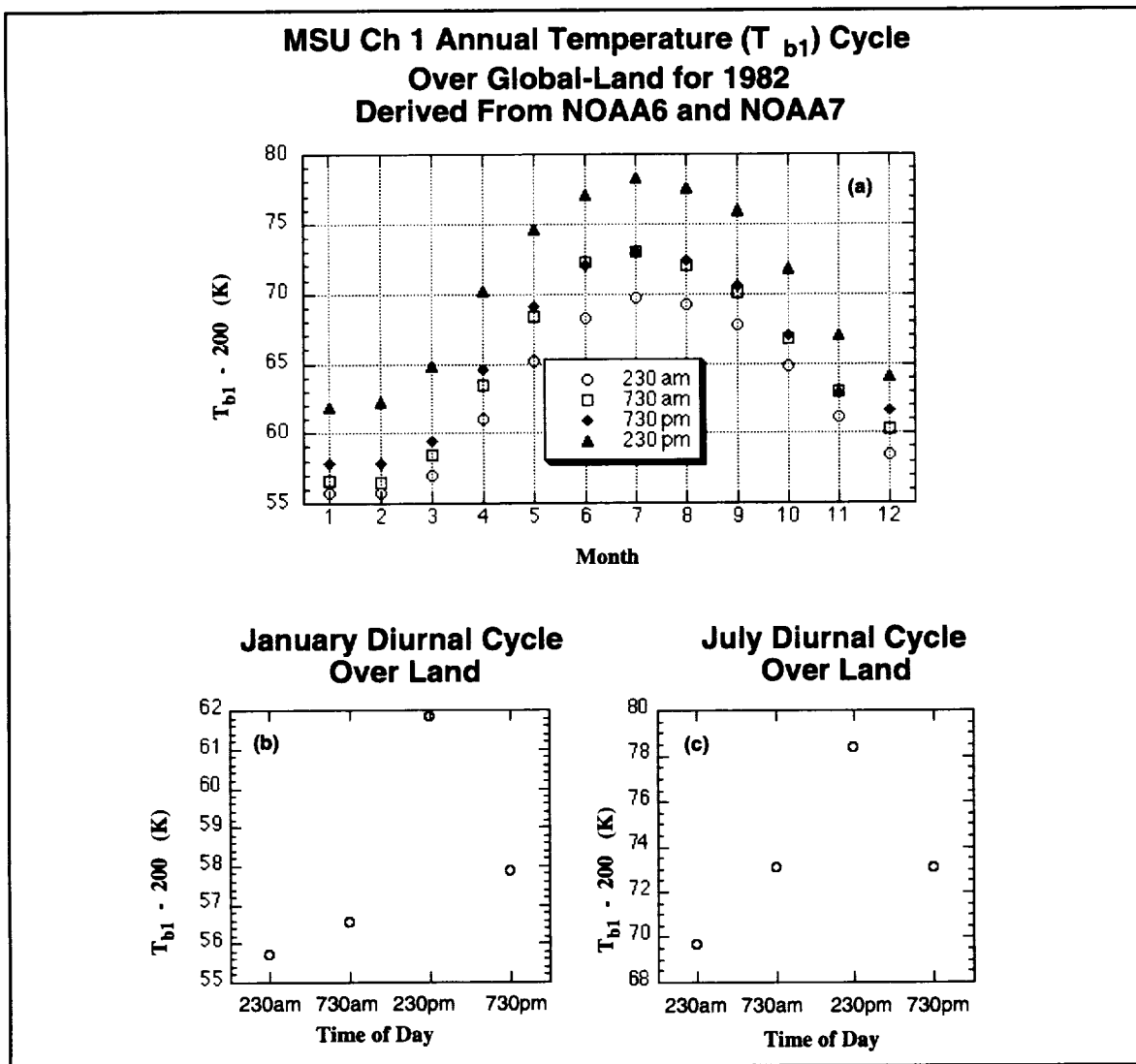
$$\bar{T}_{AM} = \frac{\sum_{i=-37}^{37} \sum_{j=1}^{120} (T_{AM})_{i,j} w_{i,j} \cos(2|i|)}{\sum_{i=-37}^{37} \sum_{j=1}^{120} w_{i,j} \cos(2|i|)} \quad (1)$$

In equation 1, $(T_{AM})_{i,j}$ is the monthly mean Ch 1 or Ch 2 temperature at the grid box (i, j) measured close to 7:30 a.m. or 2:30 a.m. The index i , when multiplied by a factor of two, represents the central latitude of the 2° latitude \times 3° longitude grid box. As i is incremented from -37 to 37, this latitude increases from -74 to 74 in steps of 2° . The grid box that has the equator as its central latitude is given by $i = 0$. The index j represents the central longitude of the grid box. As j increases from 1 to 120, the longitude increases in steps of 3° from 178.5° W to 178.5° E. Weighting by the cosine of latitude is done to get proper area average over the spherical Earth. The weight $w_{i,j}$ assigned to each grid box is normally equal to one. However, when we are estimating the global Ch 1 or Ch 2 mean temperature over lands, $w_{i,j}$ is set equal to zero for the grid boxes representing oceans and coastlines. Similarly, when we are estimating Ch 1 or Ch 2 mean temperature over oceans, $w_{i,j}$ is set equal to zero over lands and coastlines. \bar{T}_{PM} is calculated in a similar fashion from the data observed close to 2:30 p.m. and 7:30 p.m. local time. In this study, we are interested in the average of \bar{T}_{AM} or \bar{T}_{PM} over global land or ocean for time periods that are much longer than 1 month. Such an average for K number of months is given by

$$\bar{T}_{AM} = \frac{1}{K} \sum_{k=1}^K \left(\bar{T}_{AM} \right)_k \quad (2)$$

As stated previously, when we separate the 1982 overlapping MSU Ch 1 observations made by NOAA 6 and NOAA 7 into four sets based on the local equatorial crossing time, we can display graphically the annual temperature cycle over global land or ocean at four local times of the day. In figure 2a, such annual temperature cycles over the land are shown. In Ch 1, there is strong information on the surface temperature and the surface emissivity. From the four

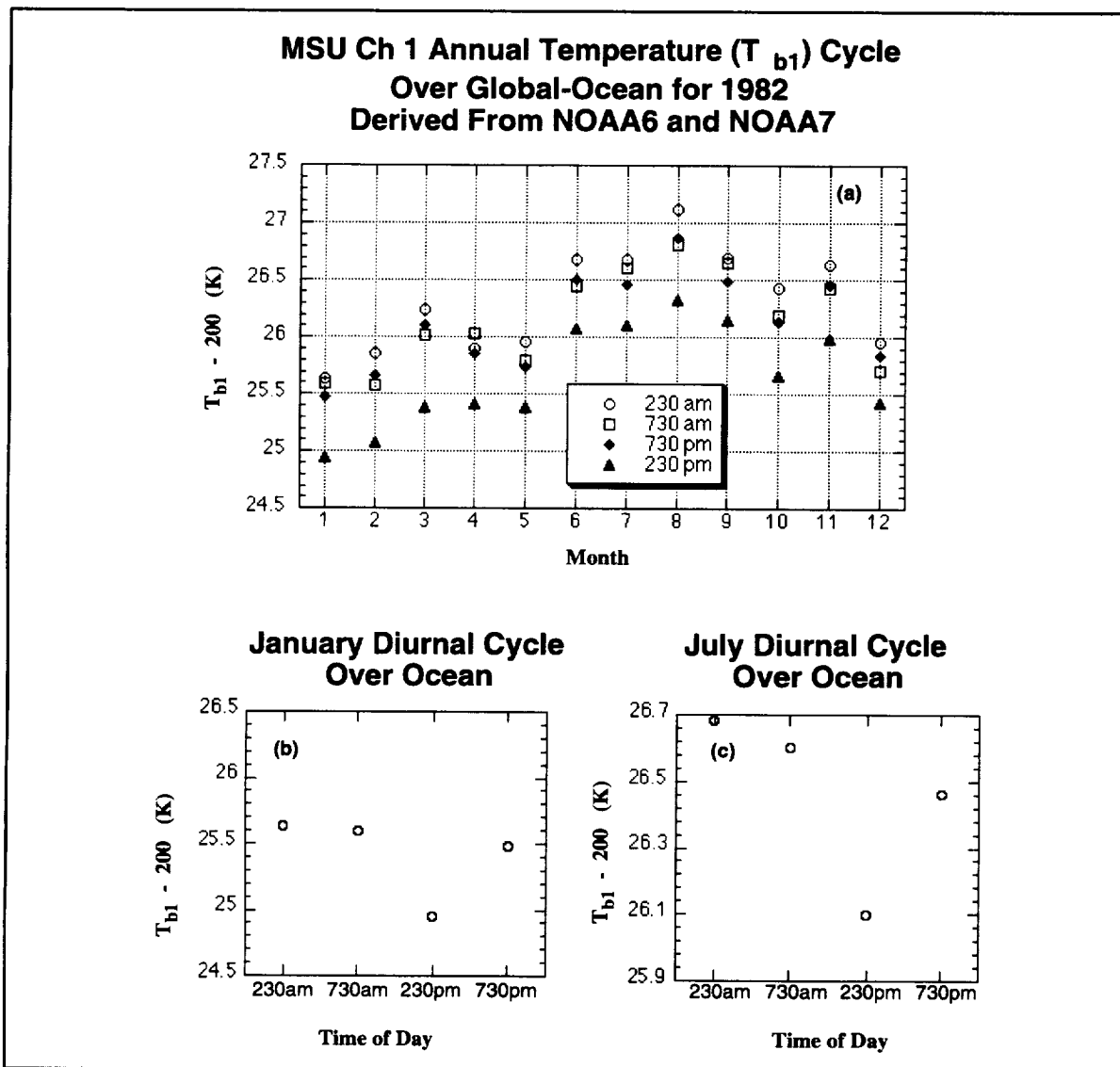
curves shown in this figure, one can get a rough estimate of the amplitude and phase of the diurnal temperature cycle for each month of the year, mainly because the amplitude of the diurnal cycle on the land, ~10 K, is large compared to the calibration errors. In figures 2b and 2c, we show the diurnal temperature cycle in January 1982 and July 1982 based on the temperature at the four local times of the day on the global land.



Figures 2a, 2b, and 2c. Annual temperature cycle over the global land for 1982 deduced from NOAA 6 in MSU Ch 1 at 7:30 a.m. and 7:30 p.m., and from NOAA 7 for the local times 2:30 a.m. and 2:30 p.m. b) Diurnal cycle over global land for January 1982, and c) for July 1982.

Similar graphical display of Ch 1 data over global ocean is presented in figures 3a, 3b, and 3c. Note that because the sea surface emissivity in the microwave region is ~ 0.5 , the brightness temperature of Ch 1 over the ocean is much smaller than that over the land. From these figures, it can also be seen that the amplitude of the diurnal cycle over ocean is small. Furthermore, we see that the MSU Ch 1 data indicates a minimum near 2 p.m., which is contrary to the Tropical Ocean Global Atmosphere-Coupled Ocean Atmosphere Response Experiment (TOGA-COARE)

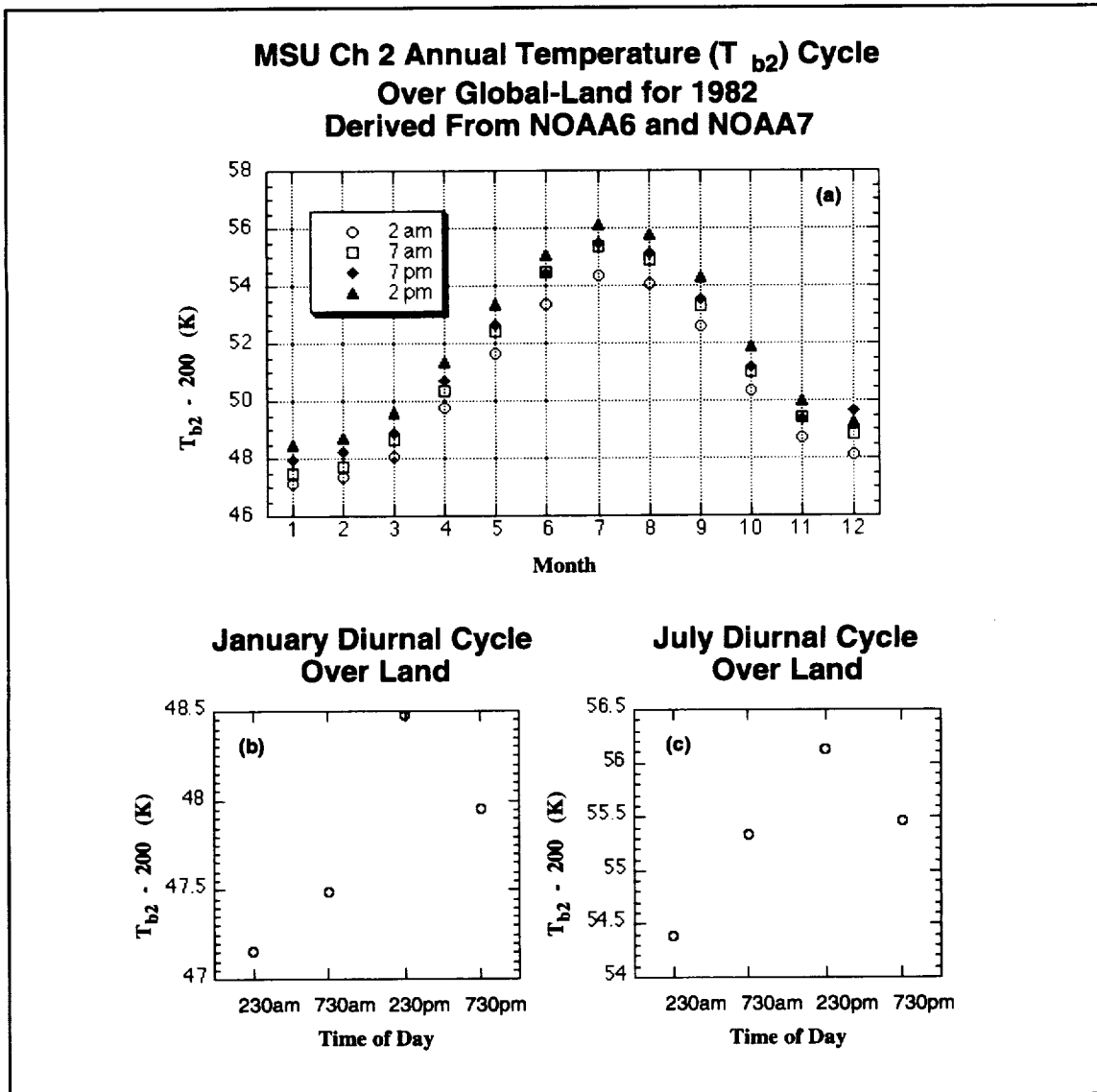
observations of the diurnal cycle over the equatorial Pacific region. TOGA-COARE observations show a maximum in the surface temperature close to 2 p.m. and the diurnal amplitude is about 1 K (Sui et al., 1997). Thus, we infer the calibration errors in Ch 1, in particular those near 2:30 p.m., are large enough (~ 0.5 K) to badly distort the weak diurnal cycle present over the oceans. Much smaller systematic calibration errors that could be present in Ch 1 data at other local times of the day are not readily noticed in figures 3b and 3c.



Figures 3a, 3b, and 3c. Same as figures 2a, 2b, and 2c, except for MSU Ch 1 data over global ocean.

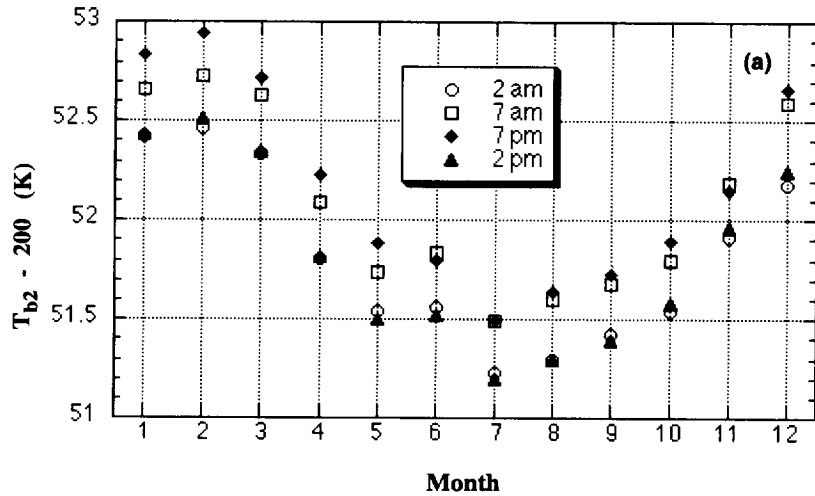
In figures 4a and 5a, we present a graphical analysis of MSU Ch 2 data on global land and ocean similar to that presented in figures 2a and 3a. The diurnal temperature cycle in Ch 2 over land and ocean in January 1982 and July 1982 are presented in figures 4b and 4c, and figures 5b and 5c, respectively. As in the Ch 1 data, the characteristics of the calibration errors can be found in the Ch 2 data. We point out that the amplitude of the diurnal cycle on the lands

in Ch 2, shown in figure 4a, is much weaker compared to that in Ch 1. The erroneous 2:30 p.m. minimum, similar to that in Ch 1, is also noticed in the diurnal cycle of Ch 2 over ocean (figures 5b and 5c). Explanation of all these systematic errors is beyond the scope of this study. However, we believe these errors could be related to instrument exposure to sunlight. Since these errors are systematic, it is possible to make suitable compensatory adjustments for them.

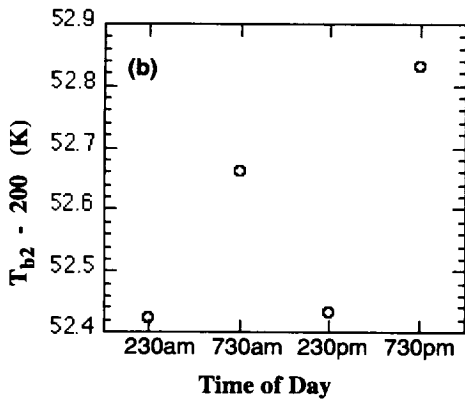


Figures 4a, 4b, and 4c. Same as figures 2a, 2b, and 2c, except for MSU Ch 2 data over global land.

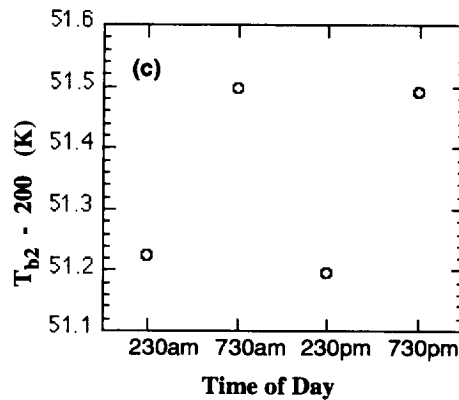
**MSU Ch 2 Annual Temperature (T_{b2}) Cycle
Over Global-Ocean for 1982
Derived From NOAA6 and NOAA7**



**January Diurnal Cycle
Over Ocean**



**July Diurnal Cycle
Over Ocean**



Figures 5a, 5b, and 5c. Same as figures 2a, 2b, and 2c, except for MSU Ch 2 data over global ocean.

Analysis of MSU Ch 1 and Ch 2 data, and the diurnal cycle presented above, could be useful also in future studies. Utilizing radiative transfer theory, we can decouple objectively the calibration errors from the diurnal cycle with the help of radiosonde observations. Such radiosonde data should correspond to the time of satellite observation and should be representative of the large footprint (~100 km) of

the radiometer. Also one should know the surface temperature and microwave surface emissivity. At this time, we do not have such measurements of the atmosphere and the surface. As an alternative, we seek a crude solution to this problem, which is elaborated in the next section. In this alternative solution, the *coupled errors* are eliminated jointly over an area of global scale.

2.3 Rectification of MSU Ch 2 data

Basically, in the MSU Ch 2 data, the annual cycle and the diurnal cycle of temperature are intertwined. These cyclical effects need to be removed. In this study, elimination of the annual cycle is treated in a simple way. This is done by averaging the data over two or three complete annual cycles. The MSU data up to the end of 1991, obtained from NOAA 6 to NOAA 11, allows us to define such multiyear averages for each satellite starting from 1 January 1980 and ending with 31 December 1991. We get global multiyear mean temperature \bar{T}_{AM} or \bar{T}_{PM} for each one of these satellites. These mean temperatures, \bar{T}_{AM} and \bar{T}_{PM} , are not adjusted for the *coupled errors*.

In table 1, we indicate for each NOAA satellite a) the satellite type, b) the local time of observations, c) the time span of observations that is used to determine global mean temperature over land and ocean at two local times of the day, and d) the months of the overlap data that are used. In table 2a, we have listed for each NOAA satellite the unadjusted global mean Ch 2 temperatures \bar{T}_{AM} and \bar{T}_{PM} , calculated according to equation 2 over global land. Similarly, in table 2b, we have listed the unadjusted global mean Ch 2 temperatures deduced over ocean. The difference in the global temperature measured at two local times of the day, $(\bar{T}_{PM} - \bar{T}_{AM})$, is also shown in these tables.

Table 1. Details of satellite data used in the present analysis.

Satellite	Satellite Type	Local Equatorial Crossing Times	Time Span of Data	Overlap Months
NOAA 6	Morning	7:30 a.m. 7:30 p.m.	Jan. 1, 1980, to Dec. 31, 1981 2 years	
NOAA 7	Afternoon	2:30 a.m. 2:30 p.m.	Jan. 1, 1982, to Dec. 31, 1984 3 years	Jan. 1982 to Dec. 1982 12 Months
NOAA 9	Afternoon	2:30 a.m. 2:30 p.m.	Jan. 1, 1985, to Dec. 31, 1986 2 years	Dec. 1984 and Jan. 1985 2 Months
NOAA 10	Morning	7:30 a.m. 7:30 p.m.	Jan. 1, 1987, to Dec. 31, 1988 2 years	Dec. 1986 and Jan. 1987 2 Months
NOAA 11	Afternoon	2:30 a.m. 2:30 p.m.	Jan. 1, 1989, to Dec. 31, 1991 3 years	Jan. 1990 to Dec. 1990 12 Months

**Table 2a. Unadjusted average Ch 2 temperature (K) data over global land.
(Add 200 to the temperature given in table.)**

Satellite	No. of Years	Ch 2 Average Unadjusted Temperature				$\bar{T}_{PM} - \bar{T}_{AM}$
		7:30 a.m.	7:30 p.m.	2:30 a.m.	2:30 p.m.	
		\bar{T}_{AM}	\bar{T}_{PM}	\bar{T}_{AM}	\bar{T}_{PM}	
NOAA 6	2	51.20	51.71			0.51
NOAA 7	3			50.53	52.04	1.49
NOAA 9	2			50.41	51.86	1.45
NOAA 10	2	51.20	51.68			0.48
NOAA 11	3			50.54	51.99	1.45

**Table 2b. Unadjusted average Ch 2 temperature (K) data over global ocean.
(Add 200 to the temperature given in table.)**

Satellite	No. of Years	Ch 2 Average Unadjusted Temperature				$\bar{T}_{PM} - \bar{T}_{AM}$
		7:30 a.m.	7:30 p.m.	2:30 a.m.	2:30 p.m.	
		\bar{T}_{AM}	\bar{T}_{PM}	\bar{T}_{AM}	\bar{T}_{PM}	
NOAA 6	2	52.04	52.26			0.22
NOAA 7	3			51.83	51.86	0.03
NOAA 9	2			51.56	51.57	0.01
NOAA 10	2	52.05	52.32			0.27
NOAA 11	3			51.68	51.66	-0.02

From table 2b, we find the difference $(\bar{T}_{pm} - \bar{T}_{am})$ of Ch 2 global ocean temperature, obtained from afternoon satellites, has a small range, -0.02 to 0.03. Also, for the morning satellites, this difference has a small range, 0.22 to 0.27. Now, if we assume the range in $(\bar{T}_{pm} - \bar{T}_{am})$ is not due to long-term variations in the diurnal temperature cycle, we can infer noise in \bar{T}_{am} or \bar{T}_{pm} . On this basis, we infer that such random noise in the 2-year or 3-year mean Ch 2 data does not exceed 0.03 K. Analysis of $(\bar{T}_{pm} - \bar{T}_{am})$ on global land, given in table 2a, also leads to a similar inference.

When there is an overlap of the data from two successive satellites in the NOAA series, we can determine the *coupled errors* in \bar{T}_{am} and \bar{T}_{pm} between those two satellites. By adjusting for the *coupled errors* in the \bar{T}_{am} data from successive satellites, we can construct a time record of the global a.m. temperature data from Ch 2 for 1980–1991. A similar global time series can be constructed for the p.m. data. In principle, from these time series, one could get the temperature change over the global ocean or global land separately for the a.m. and p.m. data sets. However, in order to enhance statistical strength in our analysis, we will combine the a.m. and p.m. data over the global land and the global ocean.

Let us assign $(\bar{T}_M)_i$ to be the unadjusted average of $(\bar{T}_{AM})_i$ and $(\bar{T}_{PM})_i$, which is given by

$$\left(\bar{T}_M\right)_i = 0.5 \times \left(\left(\bar{T}_{AM}\right)_i + \left(\bar{T}_{PM}\right)_i \right). \quad (3)$$

In this equation, the subscript i represents a number from 1 to 5 that corresponds with one of the NOAA series of satellites (6, 7, 9, 10, or 11), respectively. Also, we choose $(\Delta\bar{T}_M)_i$ to denote the difference between the average temperature of two overlapping successive satellites i and $i-1$. This can be expressed as

$$\left(\Delta\bar{T}_M\right)_i = \bar{T}_i - \bar{T}_{i-1} \text{ for } i=2 \text{ to } 5. \quad (4)$$

With the aid of these symbolisms, we can represent the adjusted average temperature $(\bar{T}_M^A)_j$ of a given satellite as

$$\left(\bar{T}_M^A\right)_j = \left(\bar{T}_M\right)_j - \sum_{i=2}^j \left(\Delta\bar{T}_M\right)_i. \quad (5)$$

In this expression, j is assigned a value from 2 to 5, which corresponds respectively with one of the NOAA series of satellites (7, 9, 10, or 11). Note that the uncorrected temperature in the series is adjusted with the sum of all of the preceding overlap errors. In table 3a, we are presenting the following global land temperature information for each satellite: \bar{T}_M ; $(-\Delta\bar{T}_M)$; $\sum_{i=2}^j (-\Delta\bar{T}_M)_i$; and \bar{T}_M^A . Similar information for ocean is presented in table 3b. Note, from tables 3a and 3b, the *coupled error* for the overlap data between NOAA 9 and NOAA 7 is nearly the same (~ 0.26) over global ocean and land. This is because $\Delta\bar{T}_M$ between these two afternoon satellites is not affected by the diurnal cycle. This is not the case for $\Delta\bar{T}_M$ of the other three satellite overlaps.

At this point, we may note that the MSU temperature \bar{T}_M^A of the global land during the 12-year period 1980–1991 is smaller than that over the ocean areas by about 0.7 K. This is simply due to the larger fractional area of ocean in the tropics as compared to that of land.

2.4 Error analysis of MSU Ch 2 data

In order to assess the amount of noise in the *coupled errors*, we present in figure 6a a plot of monthly mean brightness temperature difference vs. month, which is derived from data taken from NOAA 7 and NOAA 6 for 1982. The 12-month mean of this difference $\Delta\bar{T}_M$ for the global land is -0.015 K and for the global ocean is -0.304 K. The standard deviation of this difference over the same period is 0.084 K for global land and 0.034 K for global ocean.

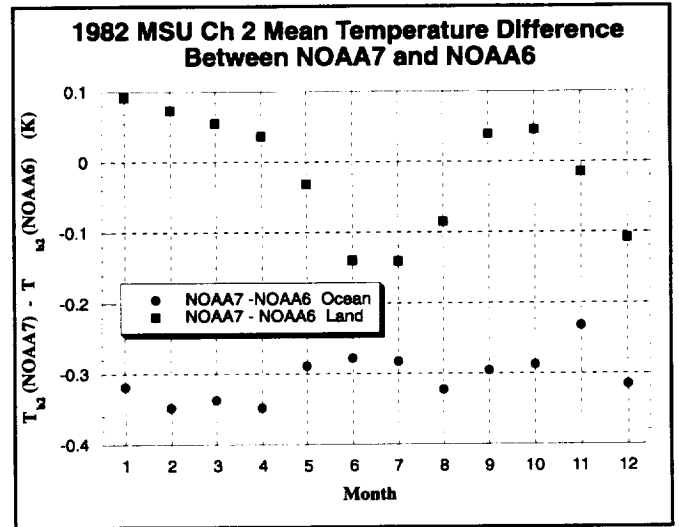


Figure 6a. Difference between MSU Ch 2 monthly mean temperature of NOAA 7 and NOAA 6 satellites, deduced from the overlap data for 1982.

Table 3a. Global land MSU Ch 2 temperature measurements and *coupled errors* (K). Included are observations before and after correction $\Sigma(-\Delta\bar{T}_m)$ for *coupled errors*. (Add 200 to the mean temperature values, \bar{T}_m and \bar{T}_m^* , given in table.)

Land				
Satellite	(\bar{T}_m)	$(-\Delta\bar{T}_m)$	$\Sigma(-\Delta\bar{T}_m)$	(\bar{T}_m^*)
NOAA 6	51.46	N/A	N/A	51.46
NOAA 7	51.28	0.015	0.015	51.30
NOAA 9	51.14	0.263	0.278	51.42
NOAA 10	51.44	0.135	0.413	51.85
NOAA 11	51.26	0.073	0.486	51.75

Table 3b. Global ocean MSU Ch 2 temperature measurements and *coupled errors* (K). Included are observations before and after correction $\Sigma(-\Delta\bar{T}_m)$ for *coupled errors*. (Add 200 to the mean temperature values, \bar{T}_m and \bar{T}_m^* , given in table.)

Ocean				
Satellite	(\bar{T}_m)	$(-\Delta\bar{T}_m)$	$\Sigma(-\Delta\bar{T}_m)$	(\bar{T}_m^*)
NOAA 6	52.15	N/A	N/A	52.15
NOAA 7	51.83	0.304	0.304	52.13
NOAA 9	51.57	0.255	0.559	52.13
NOAA 10	52.18	-0.285	0.274	52.45
NOAA 11	51.67	0.417	0.691	52.36

A similar analysis of the *coupled errors* deduced from NOAA 11 and NOAA 10 overlap data is presented for 1990 in figure 6b. The average $\Delta\bar{T}_m$ of the monthly mean brightness for 12 months is -0.073 K for global land and -0.417 K for global ocean; and the respective standard deviations are 0.074 K and 0.03 K. From figures 6a and 6b, we note that the monthly mean brightness temperature difference for global land and ocean tends to have a crude mix of annual and semi-annual cyclical patterns. We suspect that this crude pattern results from changes in the diurnal cycle of temperature. In addition, it possibly could be due to the equatorial crossing of the Sun twice a year, and thereby a dependence on the Sun-Earth geometry during the course of the year. Furthermore, the pattern on the land is weighted more heavily by the lands in the Northern Hemisphere, while the pattern over the ocean is weighted by the oceans in the Southern Hemisphere. As a result, they tend to have an opposite phase. On the other hand, the 12-month mean value of the monthly mean brightness temperature difference on land and ocean is strongly dependent on the intersatellite instrument calibration.

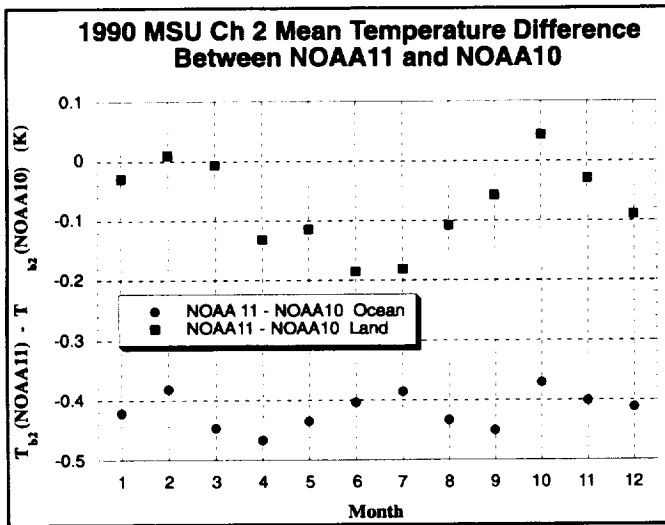


Figure 6b. Same as figure 6a, except for NOAA 11 and NOAA 10 satellites, for 1990.

The overlapping data between NOAA 9 and NOAA 7, and NOAA 10 and NOAA 9, covers a much shorter period (see table 1) and does not permit us to make annual statistical analyses as given above. For this reason, we will assume that for these two short overlap periods, the standard deviation, or the noise, introduced on an annual basis into $\Delta\bar{T}_m$ of the global land and global ocean is 0.084 K and 0.034 K, respectively. However, since each of these short overlaps spans only 2 months, we will scale upwards these noise values by a factor of $\sqrt{12 / 2}$. This scaling increases

these values to 0.206 K for the global land and to 0.083 K for the global ocean.

Assuming that the noise in $\Delta\bar{T}_m$ of the four overlap periods is random, we can calculate the effective noise in our satellite record for the long-term of 1980–1991. This effective noise in the Ch 2 temperature record calculated for the global ocean (σ_o) is 0.063 K and for the global land is 0.156 K. When these noise values are weighted appropriately for the land and ocean areas, we find an effective noise value for the globe (σ_g) is 0.103 K.

As indicated earlier, the random error in the 2-year or 3-year averages of Ch 2 temperature, deduced from each satellite in our analysis, is 0.03 K. In addition, based on the analysis of Prabhakara et al. (1995 and 1996), we assume the combined noise due to the hydrometeors and surface emissivity in these average temperatures is close to 0.05 K. Now, combining these errors with σ_o , σ_L , and σ_g yields the total error in the temperature derived for ocean, land, and the globe in the period 1980–1991. These total errors, for oceans σ_o , lands σ_L , and the globe σ_g , can be expressed as

$$\begin{aligned} \sigma_o &= \sqrt{0.03^2 + 0.05^2 + \sigma_o'^2} = \sqrt{0.03^2 + 0.05^2 + 0.063^2} \approx 0.09 \text{ K} \\ \sigma_L &= \sqrt{0.03^2 + 0.05^2 + \sigma_L'^2} = \sqrt{0.03^2 + 0.05^2 + 0.156^2} \approx 0.17 \text{ K} \quad (6) \\ \sigma_g &= \sqrt{0.03^2 + 0.05^2 + \sigma_g'^2} = \sqrt{0.03^2 + 0.05^2 + 0.103^2} \approx 0.12 \text{ K} . \end{aligned}$$

When the satellite data is divided into a.m. and p.m. subsets, the corresponding errors for these subsets will be increased substantially. For this reason, we have not done the global temperature analysis for MSU Ch 2 data for a.m. and p.m. separately.

2.5 Global temperature change and trend from MSU Ch 2:

Now, if the initial and final temperatures of the globe are respectively \bar{T}_0 and \bar{T}_f , then the global temperature trend can be deduced from the following equation:

$$\bar{T}_f = \bar{T}_0 + \int \left(\frac{dT}{dt} \right) dt = \bar{T}_0 + \left(\frac{\Delta T}{\Delta t} \right) \delta t , \quad (7)$$

where $\overline{(\Delta T / \Delta t)}$ is the average global temperature trend over the period δt . Thus,

$$\left(\frac{\Delta T}{\Delta t} \right) = \frac{\bar{T}_f - \bar{T}_0}{\delta t} . \quad (8)$$

The adjusted global ocean temperature \bar{T}_m^{\wedge} values, shown in table 3b, indicates an increase of Ch 2 temperature of about 0.21 ± 0.09 K; while on the global land, this increase is about 0.29 ± 0.17 K (table 3a). From tables 3a and 3b, we note that the corrected temperature over global land and ocean increases or decreases simultaneously during the time period 1980–1991. Finally, from the above analysis, we find that the global temperature change is 0.23 ± 0.12 K, which is based on the global mean temperature observed by Ch 2 (53.74 GHz) of MSU that is flown on each successive NOAA operational satellite from 1980 to 1991 (6, 7, 9, 10, and 11).

Note the trend estimated from equation 8 is a simple average between the initial and final data in the time series. On the other hand, the trend based on a linear regression fit will give more importance to extreme values of the data in the time series.

In figure 7, the adjusted MSU Ch 2 global temperature is shown as a function of time. In this figure, the solid lines correspond to the scale on the left ordinate and represent global mean temperature deduced from successive satellites (6, 7, 9, 10, and 11) covering the period 1980–1991. The MSU observed warming, 0.23 ± 0.12 K, from 1980 to 1991 can be readily appreciated from this figure. In figure 7, we

have also presented the time series of the MSU Ch 2 global temperature anomalies, which are shown simply to illustrate the seasonal and interannual variations. The 12-year mean annual cycle is eliminated to get this anomaly series. These satellite-derived anomalies compare well with those obtained from conventional data.

We have not considered the possible influence of the long-term stratospheric temperature change on that of Ch 2. The study of SC (1992) indicates that a decrease of about 0.3 K in the stratospheric temperature during the period 1979–1990 increases the Ch 2 temperature by only ~ 0.02 K in that period. For this reason, we have neglected this small effect.

Some NOAA satellites had drifts in their orbits, which change their equatorial crossing times. Intersatellite adjustments for *coupled errors* obtained from the overlap data of successive satellites can compensate partially for the errors in Ch 2 data due to such drifts. Also, the MSU instruments could have some degradation in their accuracy with time. Error due to degradation effect also can be remedied partially with the intersatellite adjustments for *coupled errors*. However, where there is no overlap between successive satellites, as is the case with the beginning or the ending satellite in the series, such errors will remain in the data.

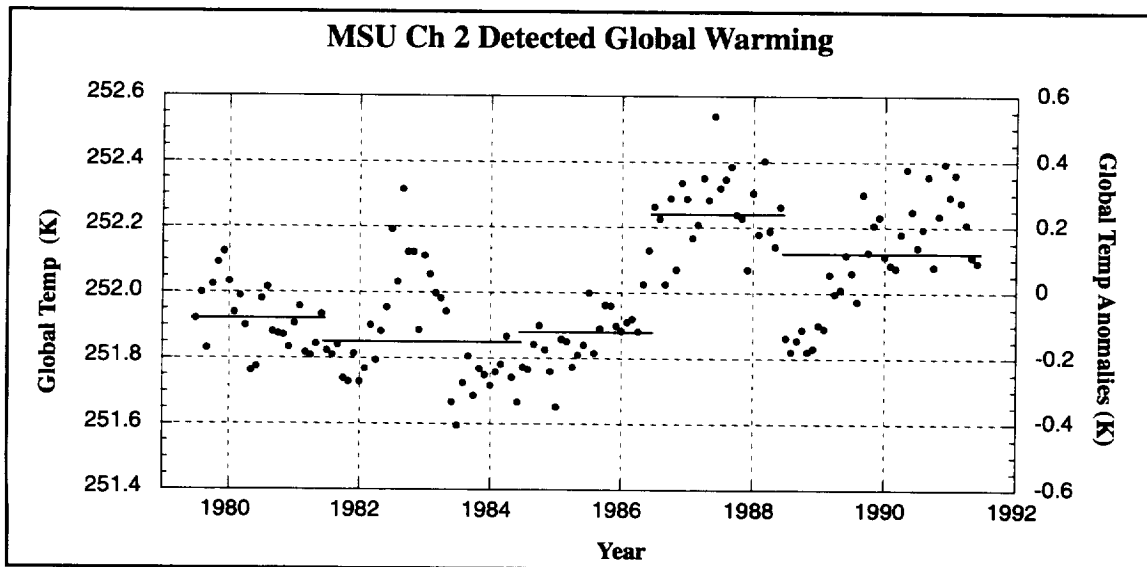


Figure 7. Corrected MSU Ch 2 global temperature as a function of time. Solid lines correspond to the scale on the left ordinate and represent global mean temperature deduced from successive satellites (6, 7, 9, 10, and 11) covering the period 1980–1991. The MSU-observed warming from 1980–1991 is 0.23 ± 0.12 K (refer to text). Open circles correspond to the scale on the right ordinate and denote monthly temperature anomalies with respect to the 12-year mean annual cycle.

3. CONCLUSIONS

Systematic calibration errors, present in the MSU Ch 2 data sets collected from sequential, polar-orbiting, Sun-synchronous NOAA operational satellites, are coupled to the diurnal temperature cycle over the globe. Since these *coupled errors* in MSU data differ between successive satellites, it is necessary to make compensatory adjustments to these multisatellite data sets in order to determine long-term global temperature change. With the aid of the observations during overlapping periods of successive satellites, we can determine such adjustments. The long-term time series of MSU Ch 2 global temperature adjusted in this fashion can yield global temperature trend.

The error in the MSU Ch 2 global mean temperature, derived from each NOAA operational satellite, is ~ 0.03 K. We arrive at this estimate based on the analysis of the difference between \bar{T}_{m} and \bar{T}_{am} , which corresponds to 2-year or 3-year averages of the MSU Ch 2 temperature over the global ocean and land (see tables 2a and 2b). The errors in the intersatellite adjustments that compensate for *coupled errors*, estimated from 12 months of overlap data between successive satellites, are about 0.034 K for global ocean and 0.084 K for global land areas. These errors are magnified when the overlap period is shorter. Such errors from short overlap periods, present in the Ch 2-derived temperature

time series, effect adversely the accuracy of the estimates of long-term global temperature change. The combined error in the 1980–1991 global temperature record is ~ 0.12 K. This combined error results from a) error in the Ch 2 estimate of global mean temperature from each satellite, b) error introduced by hydrometeors and surface contamination, and c) *coupled errors* from each overlap of successive satellites.

The global temperature change is estimated from a series of 2-year or 3-year averages of Ch 2 global temperature, which have been adjusted for coupled diurnal effects and intersatellite instrument calibration errors. We find such temperature change from 1980 to 1991 for the global ocean is 0.21 ± 0.09 , for the global land 0.29 ± 0.17 , and on the combined global land and ocean region 0.23 ± 0.12 .

The advantages of the method of analysis developed here stem from our ability to separate the MSU data based on the two local equatorial crossing times of each satellite. This, together with the analysis of Ch 1 and Ch 2 temperature data (not the temperature *anomalies*), allows us to understand and to determine explicitly the *coupled errors* on the global land and ocean. Also, since the estimations of warming, performed separately for the global ocean and global land, are found to be consistent with each other, confidence is reinforced in our method of analysis and its results.

REFERENCES

1. Angell, J.K., 1988: Variations and Trends in Tropospheric and Stratospheric Global Temperatures, 1958–87. *J. Climate*, **1**, 1296–1313.
2. Hanson, J. and H. Wilson, 1993: Commentary on the Significance of Global Temperature Records. *Climatic Change*, **25**, 185–191.
3. Hurrell, J. W. and K. E. Trenberth, 1996: Satellite Versus Surface Estimates of Air Temperature Since 1979. *J. Climate*, **9**, 2222–2232.
4. NOAA, 1997: *NOAA Polar–Orbiter Data Users Guide*. (Available from NOAA/NESDIS/NCDC/CSD/SSB, FOB, Room G233, E/C C33, 4700 Suitland Road, Suitland, MD, 20746 or www2.ncdc.gov/POD/podug/cover.htm)
5. Prabhakara C., J. J. Nucciarone and J.–M. Yoo, 1995: Examination of Global Atmospheric Temperature Monitoring With Satellite Microwave Measurements 1) Theoretical Consideration. *Climatic Change*, **30**, 349–366.
6. Prabhakara C., J.–M. Yoo, S. P. Maloney, J. J. Nucciarone, A. Arking, M. Cadeddu and G. Dalu, 1996: Examination of Global Atmospheric Temperature Monitoring with Satellite Microwave Measurements 2) Analysis of Satellite Data. *Climatic Change*, **33**, 459–476.
7. Shah, P. K. and D. Rind, 1995: Use of Microwave Brightness Temperatures with a General Circulation Model. *J. Geophys. Res.*, **100**, 13841–13874.
8. Spencer, R. W. and J. R. Christy, 1990: Precise Monitoring of Global Temperature Trends From Satellites. *Science*, **247**, 1558–1562.
9. ———, 1992: Precision and Radiosonde Validation of Gridpoint Temperature Anomalies, Part II: A Tropospheric Retrieval and Trends During 1979–90. *J. Climate*, **5**, 858–866.
10. Spencer, R. W., J. R. Christy and N. C. Grody, 1991: Precision Tropospheric Temperature Monitoring 1979–1990. *Global and Planetary Change*, **90**, 113–120.
11. Sui, C.–H., K.–M. Lau, Y. Takayabu and D. Short, 1997: Diurnal Variations in Tropical Oceanic Cumulus Convection During TOGA–COARE. *J. Atmos.*, **54**, 639–654.

REPORT DOCUMENTATION PAGE

Form Approved
OMB No. 0704-0188

Public reporting burden for this collection of information is estimated to average 1 hour per response, including the time for reviewing instructions, searching existing data sources, gathering and maintaining the data needed, and completing and reviewing the collection of information. Send comments regarding this burden estimate or any other aspect of this collection of information, including suggestions for reducing this burden, to Washington Headquarters Services, Directorate for Information Operations and Reports, 1215 Jefferson Davis Highway, Suite 1204, Arlington, VA 22202-4302, and to the Office of Management and Budget, Paperwork Reduction Project (0704-0188), Washington, DC 20503.

1. AGENCY USE ONLY (Leave blank)		2. REPORT DATE January 1998	3. REPORT TYPE AND DATES COVERED Technical Memorandum	
4. TITLE AND SUBTITLE Global Warming Estimation From MSU			5. FUNDING NUMBERS 913	
6. AUTHOR(S) C. Prabhakara, R. Iacovazzi Jr., J.-M. Yoo and G. Dalu				
7. PERFORMING ORGANIZATION NAME(S) AND ADDRESS (ES) Climate and Radiation Branch Laboratory for Atmospheres Goddard Space Flight Center Greenbelt, Maryland 20771			8. PERFORMING ORGANIZATION REPORT NUMBER 98A00404	
9. SPONSORING / MONITORING AGENCY NAME(S) AND ADDRESS (ES) National Aeronautics and Space Administration Washington, DC 20546-0001			10. SPONSORING / MONITORING AGENCY REPORT NUMBER TM-1998-206646	
11. SUPPLEMENTARY NOTES Iacovazzi: Raytheon STX Corporation, Yoo: Ewha Womans University Dalu: CNR				
12a. DISTRIBUTION / AVAILABILITY STATEMENT Unclassified - Unlimited Subject Category: 47 Report available from the NASA Center for AeroSpace Information, 800 Elkridge Landing Road, Linthicum Heights, MD 21090; (301) 621-0390.			12b. DISTRIBUTION CODE	
13. ABSTRACT (Maximum 200 words) Microwave Sounding Unit (MSU) Ch 2 data sets, collected from sequential, polar-orbiting, Sun-synchronous National Oceanic and Atmospheric Administration operational satellites, contain systematic calibration errors that are coupled to the diurnal temperature cycle over the globe. Since these <i>coupled errors</i> in MSU data differ between successive satellites, it is necessary to make compensatory adjustments to these multisatellite data sets in order to determine long-term global temperature change. With the aid of the observations during overlapping periods of successive satellites, we can determine such adjustments and use them to account for the <i>coupled errors</i> in the long-term time series of MSU Ch 2 global temperature. In turn, these adjusted MSU Ch 2 data sets can be used to yield global temperature trend. In a pioneering study, Spencer and Christy (SC) (1990) developed a procedure to derive the global temperature trend from MSU Ch 2 data. Such a procedure can leave unaccounted residual errors in the time series of the temperature <i>anomalies</i> deduced by SC, which could lead to a spurious long-term temperature trend derived from their analysis. In the present study, we have developed a method that avoids the shortcomings of the SC procedure.				
14. SUBJECT TERMS Microwave Sounding Unit (MSU) Ch 2 data, global temperature change, remote sensing.			15. NUMBER OF PAGES 25	
			16. PRICE CODE	
17. SECURITY CLASSIFICATION OF REPORT Unclassified	18. SECURITY CLASSIFICATION OF THIS PAGE Unclassified	19. SECURITY CLASSIFICATION OF ABSTRACT Unclassified	20. LIMITATION OF ABSTRACT UL	